Ice formation in unsaturated frozen soils

Y. Mao, E. Romero & A. Gens

Department of Civil and Environmental Engineering, Universitat Politècnica de Catalunya, Barcelona, Spain

ABSTRACT: This paper presents a procedure for determining unfrozen water saturation in a partially saturated frozen soil (clayey silt) using bulk electrical conductivity (EC) measurements. A modification of Archie's law is proposed to describe the relationship between soil bulk EC, temperature, porosity and degree of unfrozen water saturation. Compacted samples have been prepared at a dry density around 1.90 Mg/m3 and at different degrees of saturation. Samples have been then subjected to freezing paths up to -15 °C. Measurements of bulk EC along the temperature decrease and freezing paths have been used to calibrate parameters associated with the proposed model. These calibrated models allow determining the amount of ice content for a given state of the partially saturated soil (porosity, initial degree of water saturation and temperature). The soil freezing retention curve has been also estimated by combining the Clausius-Clapeyron equation with water retention data on drying. A good agreement has been observed between the estimation based on EC measurements and results from water retention data, which validates the proposed procedure.

1 INTRODUCTION

Ice content and its migration process have not been extensively studied in partially saturated soils (Liu and Si 2011, Zhou et al. 2014), despite having important practical applications on geocomposite capillary barriers used to reduce frost heave in soils, on artificial ground freezing in partially saturated soils and on engineered barriers that are subjected to freezing and thawing processes.

To experimentally validate coupled THM models for frozen soils (see for instance, Nishimura et al. 2009, Casini et al. 2016), cryogenic suction is an important stress variable to determine together with ice content. Nevertheless, as cryogenic suction is usually difficult to be measured, experimental efforts have been mainly concentrated in estimating ice content (or unfrozen water content) and the soil freezing retention curve (SFRC). Several procedures have been proposed to determine ice content in frozen soils, which include calorimeter technique (Williams 1964), time domain reflectometry TDR (Patterson and Smith 1981, Watanabe and Wake 2009, Mao et al. 2016), nuclear magnetic resonance (Smith and Tice 1988), heat pulse probe (Liu and Si 2011), and combined gamma ray attenuation and TDR (Zhou et al. 2014), to cite some of the most used techniques.

At the same time, empirical and theoretical models have been developed to interpret these indirect experimental results, and thus better assess the unfrozen water content at a given state of initial water content (volumetric / gravimetric) and temperature (Dillon and Anderson 1966, Anderson and Tice 1972, Liu and Yu 2013, Mu 2017). However, in most of the previously cited models, the information on porosity and initial degree of water saturation has not been usually considered. Konrad (1990) measured the SFRC of clayey silt at different void ratios, which highlighted the important porosity effects on the unfrozen water retention properties.

In this paper, an electrical set-up with cooling bath has been used to measure the bulk electrical conductivity (EC) properties at different temperatures (from 20°C to -15°C) of a partially saturated clayey silt. Archie's law has been modified to consider temperature effects on bulk EC. Furthermore, a new empirical model has been proposed to estimate the unfrozen water content at a given state of porosity, initial degree of saturation and temperature. To validate the proposed approach, the SFRC has been also estimated by combining the Clausius-Clapeyron equation with water retention data on drying.

2 MATERIALS AND METHODS

2.1 *Test setup*

A small Perspex cell (25.5 mm in inner diameter and 30 mm high) and presented in Figure 1 is used to measure the EC at different temperatures using a cooling bath (Mao 2018). A uniform flow of electric current is applied on both ends of the sample (plate electrodes 'c' in the figure), and the EC is determined from voltage readings using a pair of needle electrodes placed in the middle of the sample ('d' in the figure). A thermocouple is inserted close to the parallel needle electrodes to measure the temperature. The calibrated electrical resistivity measurement system is from the Geotechnical Engineering Laboratory at Politecnico di Torino (see Comina et al. 2008).

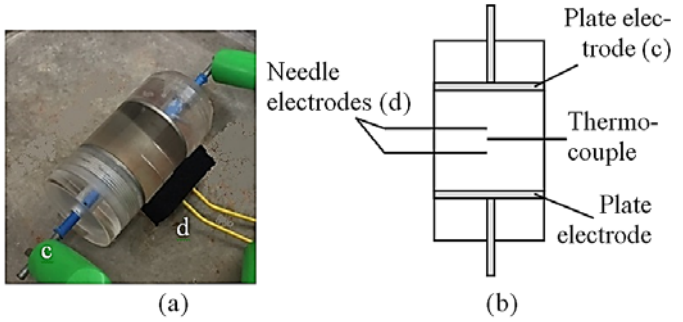

Figure 1. (a) Experimental set-up and (b) schematic of small cell for measuring EC of frozen soils.

2.2 *Soil properties*

Barcelona clayey silt is used in this research. The maximum particle size is limited to 2 mm due to the experimental set-up used. Selected properties are summarised in Table 1.

Table 1. Selected properties of the clayey silt.

Soil properties	
Density of solids, ρ_s (Mg/m^3)	2.67
Liquid limit (%)	28 to 31
Plastic limit (%)	19
Silty fraction between 2 and 75 μm (%)	40 to 46
Clay-size fraction ≤ 2 μm (%)	13 to 19

Water retention data on drying path and in terms of degree of saturation S_r are shown in Figure 2. The van Genuchten (1980) expression is used to fit the data:

$$S_r = \left[1+\left(\frac{s}{P}\right)^{\frac{1}{1-\lambda}}\right]^{-\lambda} \quad (1)$$

where s is suction, λ=0.26 is a material parameter and P=0.46 MPa is associated with the air entry value.

2.3 *Properties of interstitial water*

A 5% NaCl solution (mass basis) is used as interstitial water instead of pure water, to better discriminate EC values between ice and unfrozen water. Figure 3 shows EC values of the solution along temperature decrease and freezing paths. A clear dependence on temperature is observed because of changes in ionic mobility and solution viscosity. It is interesting to detect that the relationship between electrical conductivity and temperature in unfrozen state (without phase change) is linear and it changes to non-linear below freezing point because of ice generation. The freezing point of 5% NaCl solution is around -3.2 °C calculated from Blagden's law for dilute solutions.

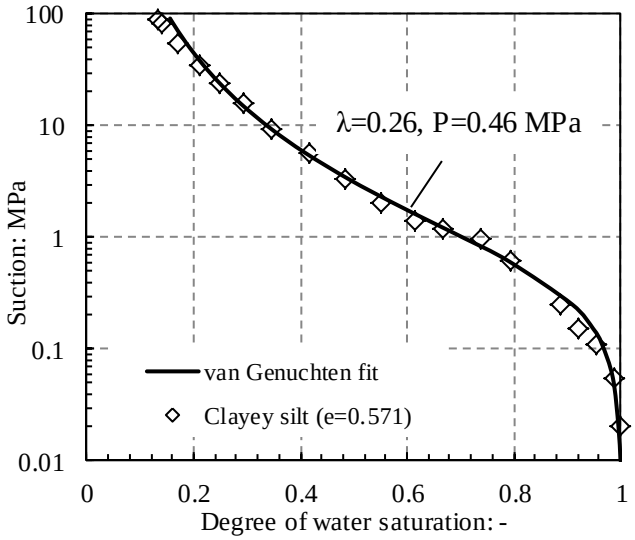

Figure 2. Water retention curve of clayey silt on drying (adapted from results by Mora 2016).

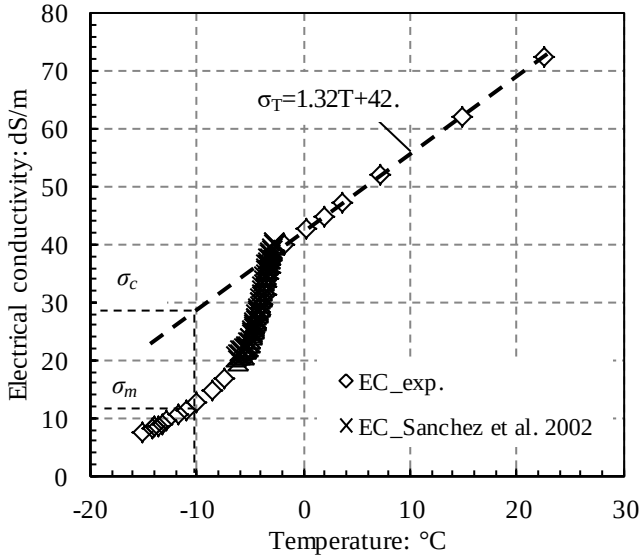

Figure 3. EC values of 5% NaCl solution along temperature decrease and freezing paths (including results along a freezing path from Sánchez et al. 2002).

It is assumed that only the liquid phase is contributing to EC, since this value in ice is approximately three orders of magnitude lower than liquid water (ionic mobility is restricted by ice lattice). For the linear part, a simple equation can be used to fit EC data of the solution with temperature:

$$\sigma_T(T) = 1.32T + 42.45 \quad (2)$$

where σ_T is the electrical conductivity of the solution (dS/m) and T the temperature (°C).

In the frozen branch of the curve, the difference in EC between extrapolated (linear extrapolation) and measured values is associated with ice formation. At freezing point, the unfrozen water saturation S_l is still equal to 1. At nearly full ice condition (S_l close to 0), the measured EC will tend to zero. Therefore, the following expression can be proposed for S_l:

$$S_l = \frac{\sigma_m}{\sigma_c} \quad (3)$$

where σ_m is the measured EC of the ice / liquid solution (dS/m), and σ_c is the extrapolated electrical conductivity from Equation 2. These values are indicated in Figure 3.

The proposed Equation 3 has been validated by comparing with reported results from Sánchez et al. (2002) for ice concentration in 5% NaCl solution (Mao 2018). Results from Sánchez et al. (2002) has been also included in Figure 3, in which a good agreement with data from this study can be observed in relation to the evolution of EC with temperature in the freezing zone.

3 EXPERIMENTAL RESULTS

The clayey silt samples have been statically compacted at different initial degrees of saturation S_{ri} and at a dry density ρ_d around 1.90 Mg/m^3. The target dry density is close to the maximum dry density of Standard Proctor (ρ_d=1.92 Mg/m^3 at S_r=0.87). The compacted state of the samples is summarised in Table 1.

The bulk EC of the samples has been measured along a temperature decrease and freezing path (from 20°C to -15°C). Figure 4a shows the evolution of bulk EC of the three samples along the temperature decrease path without phase change. A linear variation of bulk EC with temperature is obtained, which is consistent with previous results for the interstitial water. It is a consequence of the very low EC of the mineral particles (primarily based on electron movement) relative to the EC of the electrolyte (based on ionic movement). Figure 4b presents the bulk EC drop of the different samples associated with the freezing stage.

Table 1. Selected physical characteristics of tested samples

Sample	Dry density ρ_d / Mg/m^3	Porosity n / -	Initial degree of saturation S_{ri} / -
1	1.90	0.282	0.730
2	1.92	0.275	1.000
3	1.87	0.293	0.859

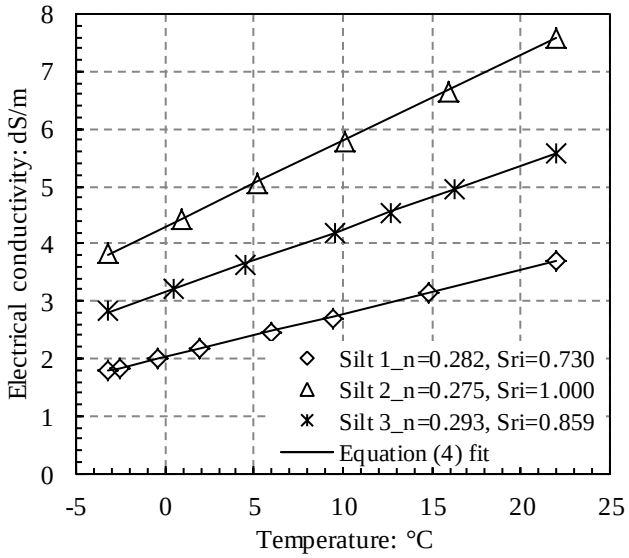

(a)

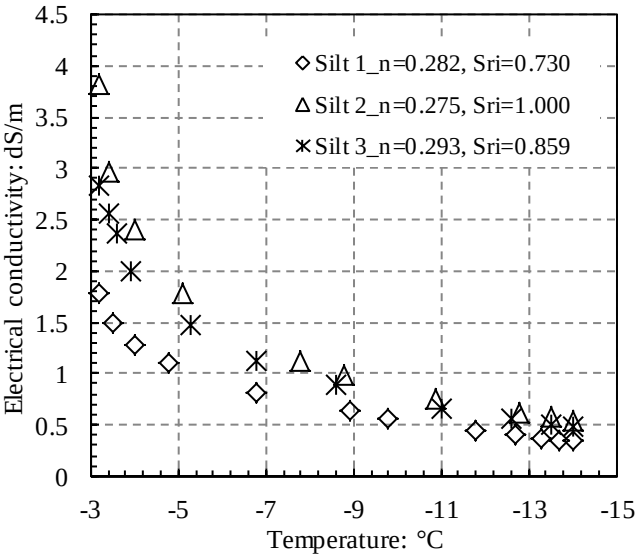

(b)

Figure 4. Soil bulk EC changes along the temperature decrease and freezing paths: (a) above freezing point; (b) below freezing point.

4 DISCUSSION

4.1 *Unfrozen water saturation*

Archie (1942) proposed a simple empirical model to link the bulk EC, σ, of sand and sandstone samples to porosity under saturated conditions. When extended to unsaturated soils, the expression can be written as (Hauck 2002):

$$\sigma = \sigma_w n^p S_{ri}^q \quad (4)$$

where σ_w is the EC of interstitial water, n the porosity, and S_{ri} is the initial degree of water saturation. p is an exponent that can be related to soil structure (usually between 1.4 and 2.0) and q is a saturation exponent, typically around 2.0.

By considering the temperature dependence of the interstitial water (Equation 2), the bulk EC of the soil (Equation (4)) at different temperatures without phase change σ_c can be described by:

$$\sigma_c = \sigma_T(T)\, n^p S_{ri}^q = (1.32T + 42.45)\, n^p S_{ri}^q \quad (5)$$

Equation 5 is used to fit test results without phase change in Figure 4a. The 1:1 scatter plot of measured bulk EC values and calculated EC values is presented in Figure 5, which displays an adequate agreement. The fitted model parameters are p=1.85 and q=2.08, which agree well with usual values adopted for Archie's law.

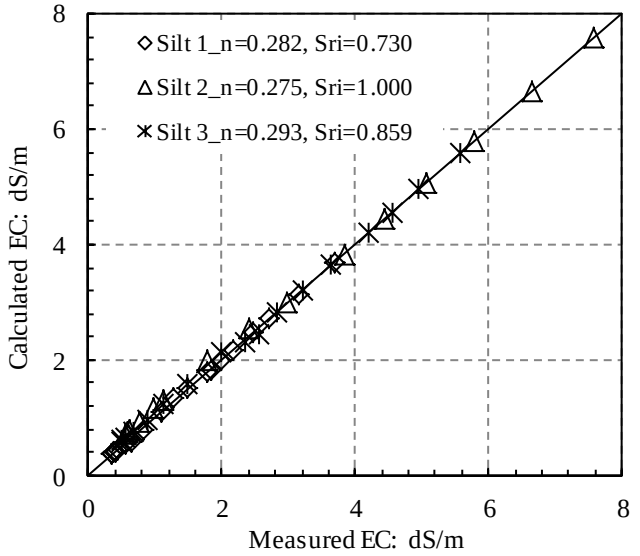

Figure 5. Scatter plot of measured EC vs calculated EC along the temperature decrease path without phase change.

It is assumed that the porosity and the total mass of water (associated with S_{ri}) do not change along soil freezing and thawing paths. The unfrozen water saturation S_l in partially saturated soils would be similar to Equation 3, but using the extended Archie's law and corrected by the initial water saturation S_{ri}, which can be rearranged as follows:

$$S_l = S_{ri}\frac{\sigma_m}{\sigma_c} = \frac{\sigma_m}{\sigma_T(T)}\, n^{-p} S_{ri}^{1-q} \quad (6)$$

A detailed derivation and validation of Equation 6 is explained in Mao (2018). Thus, the unfrozen water saturation in the partially saturated clayey silt can be obtained as:

$$S_l = \frac{\sigma_m n^{-1.85} S_{ri}^{-1.08}}{1.32T + 42.45} \quad (7)$$

The evolution of the unfrozen water saturation with temperature of the three soil samples are plotted in Figure 6. Ice formation starts at around -3.2°C due to salinity effects. At the beginning, ice generates quite fast with small temperature drops. Nevertheless, at temperatures below -7ºC the evolutions of the unfrozen water saturation of the three samples tend to converge to a residual value despite starting from different initial degrees of saturation. When compared to published results on natural frozen clayey silts with lower salinity of the interstitial water, the current results tend to display higher unfrozen water saturations at specified temperatures (Mao 2018). The salinity not only affects the freezing point, but also the residual unfrozen water content (Watanabe and Mizoguchi 2002, Xiao et al. 2018).

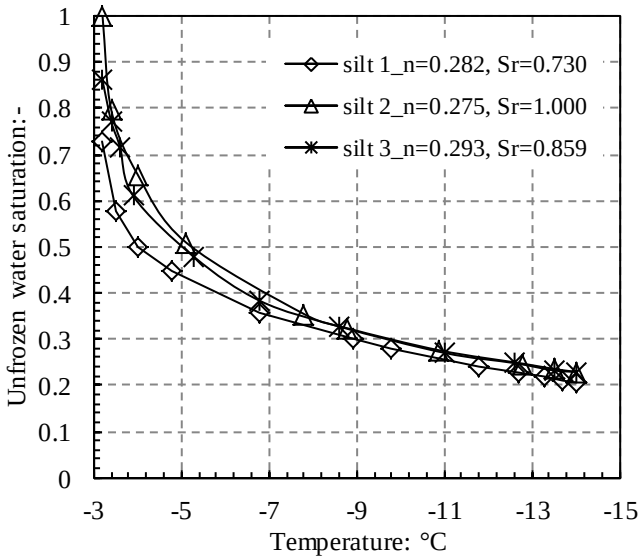

Figure 6. Estimated unfrozen water saturations with temperature for samples starting at different initial degrees of saturation.

4.2 *Soil freezing retention curve*

The approach followed to determine the evolution of the unfrozen water saturation with temperature has been validated using the water retention data on drying presented in Figure 2. To express the data in terms of pressures (cryogenic suction) as in the water retention curve (suction), several researchers have used the Clausius-Clapeyron equation (see for instance, Nishimura et al. 2009, Lebeau et al. 2012). This equation rules the thermodynamic requirement for the equilibrium coexistence (equilibrium of the chemical potential) of two phases (liquid water and ice phases):

$$\mathrm{d}P_i = \frac{\rho_i}{\rho_l}\,\mathrm{d}P_l - \frac{\rho_i\, l}{T}\,\mathrm{d}T \quad (8)$$

where ρ is the density, T the absolute temperature, P the absolute pressure, and l=333.5 kJ/kg the specific latent heat of fusion of water. Subscripts l and i refer to liquid water and ice, respectively. The differential form can be integrated using atmospheric pressure

and freezing temperature T_f as references. Since ρ_i/ρ_l is close to 1, the equation reduces to:

$$P_i - P_l = -\rho_i \, l \, \ln\left(\frac{T}{T_f}\right) \tag{9}$$

The non-wetting ice invasion at P_i-P_l can be assumed to be equivalent to air intrusion at matric suction s during a drying path for the same diameter of pores x:

$$s = \frac{4\sigma_l \cos\theta_l}{x} \;;\; P_i - P_l = -\frac{4\sigma_i \cos\theta_i}{x}$$
$$P_i - P_l = -\frac{\sigma_i \cos\theta_i}{\sigma_l \cos\theta_l} s \approx 0.45\, s \tag{10}$$

where σ_l=0.073 N/m is the surface tension of liquid water at 20ºC and $\cos\theta_l$=1 the wetting coefficient for the air-water interface. σ_i=0.033 N/m is the surface tension of ice, $\cos\theta_i$ the wetting coefficient for the ice-water interface ($\theta_i \approx 180º$, see for instance Knight 1971), and x the entrance pore diameter for a cylindrical model.

The degree of saturation at a certain suction, assuming non-deformable soil, is used to evaluate the unfrozen water saturation corresponding to the equivalent P_i-P_l determined using Equation 10.

Figure 7 shows the estimated soil freezing retention curve SFRC from water retention data compared to the previous results starting at S_{ri}=1.0. A very good agreement is observed between both results, which give confidence to the approach followed to estimate the unfrozen degree of saturation by bulk EC readings.

The figure also includes the SFRC estimated from mercury intrusion porosimetry MIP results on a freeze-dried sample at n=0.293. A similar procedure has been followed, in which the non-wetting mercury intrusion has been assumed to be equivalent to ice invasion and the degree of saturation of non-wetting mercury has been used to evaluate the unfrozen water saturation. Furthers details are explained in Mao (2018). The SFRC based on MIP results also displays a consistent trend with previous results, although ice generates faster with small temperature drops close to the freezing point.

5 CONCLUDING REMARKS

The bulk EC of statically compacted clayey silt at three different initial degrees of saturation has been measured along temperature decrease and freezing paths (from 20°C to -15°C). A 5% NaCl solution has been used as interstitial water to better discriminate EC values between ice and unfrozen water. Archie's law together with a temperature dependent expression for the EC of the interstitial water in the freezing zone has been used to interpret the experimental results and estimate the unfrozen water content at different temperatures. The proposed approach considers the porosity effects and the initial degree of saturation. Salinity of the interstitial water affects the freezing point, as well as the residual unfrozen water saturation below -7ºC.

The unfrozen water results from bulk EC measurements have been compared with the SFRC obtained by combining the Clausius-Clapeyron equation with water retention data on drying, as well as with mercury intrusion porosimetry results. Very good agreement has been found between the proposed approach using bulk EC data and the experimental data from the water retention curve.

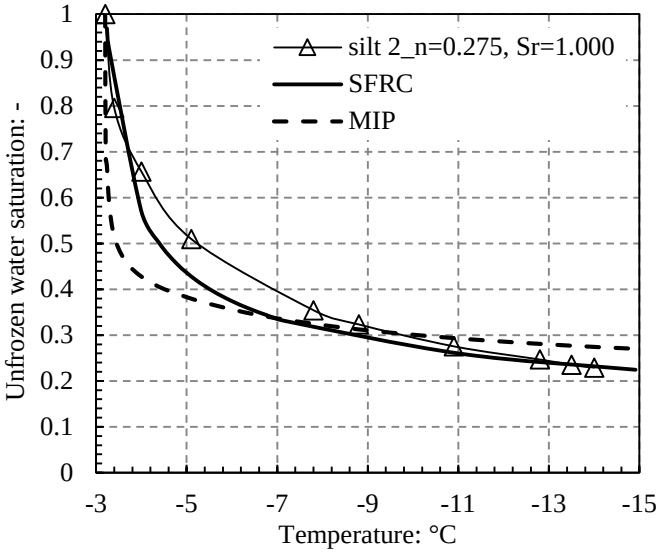

Figure 7. Estimated unfrozen water saturation for sample starting at full saturation. SFRCs based on combined Clausius-Clapeyron equation and water retention / mercury intrusion porosimetry data.

6 ACKNOWLEDGEMENTS

Special thanks to Prof. Guido Musso (Politecnico di Torino) for his help with the electrical resistivity tomography tests. The first author acknowledges the financial support from China Scholarship Council (CSC).

7 REFERENCES

Anderson, D.M. & Tice, A.R. 1972. Predicting unfrozen water contents in frozen soils from surface area measurements. *Highway Research Record* 393: 12-18.

Archie, G.E. 1942. The electrical resistivity log as an aid in determining some reservoir characteristics. *Transactions of the AIME* 146(1): 54-62.

Casini, F., Gens, A., Olivella, S. & Viggiani, G. 2016. Artificial ground freezing of a volcanic ash: laboratory tests and modelling. *Environmental Geotechnics* 3(3): 1-14.

Comina, C., Romero, E., Musso, G. & Foti, S. 2008. EIT Oedometer: an advanced cell to monitor spatial and time variability in soil with electrical and seismic measurements. *Geotechnical Testing Journal*, ASTM 31(5): 1-9.

Dillon, H.B. & Andersland, O.B. 1966. Predicting unfrozen water contents in frozen soils. *Canadian Geotechnical Journal* 3(2): 53-60.

Hauck, C. 2002. Frozen ground monitoring using DC resistivity tomography. *Geophysical Research Letters* 29(21): 1-4.

Knight, C.A. 1971. Experiments on the contact angle of water on ice. *Philosophical Magazine* 23(181): 153-165.

Konrad, J.M. 1990. Unfrozen water as a function of void ratio in a clayey silt. *Cold Regions Science and Technology* 18(1): 49-55.

Lebeau, M. & Konrad, J.M. 2012. An extension of the capillary and thin film flow model for predicting the hydraulic conductivity of air-free frozen porous media. *Water Resources Research* 48: W07523.

Liu, G. & Si, B. 2011. Soil ice content measurement using a heat pulse probe method. *Canadian Journal of Soil Science* 91(2): 235-246.

Liu, Z. & Yu, X. 2013. Physically based equation for phase composition curve of frozen soils. *Transportation Research Record: Journal of the Transportation Research Board* 2349: 93-99.

Mao, Y., Romero E. & Gens A. 2016. Exploring ice content on partially saturated frozen soils using dielectric permittivity and bulk electrical conductivity measurements. *E3S Web of Conferences* 9: 07005.

Mao, Y. 2018. Study of ice content and hydro-mechanical behaviour of frozen soils. *PhD thesis, Universitat Politècnica de Catalunya, Spain.*

Mora, R.S. 2016. Efectos de la microestructura en el comportamiento hidromecánico de suelos compactados. *PhD thesis, Universitat Politècnica de Catalunya, Spain.*

Mu, Q. 2017. Hydro-mechanical behaviour of loess at elevated and sub-zero temperatures. *PhD thesis, University of Science and Technology, Hong Kong.*

Nishimura, S., Gens, A., Olivella, S. & Jardine, R.J. 2009. THM coupled finite element analysis of frozen soil: formulation and application. *Géotechnique* 59(3): 159-171.

Patterson, D.E. & Smith, M.W. 1981. The measurement of unfrozen water content by time domain reflectometry: Results from laboratory tests. *Canadian Geotechnical Journal* 18(1): 131-144.

Sánchez, R.I., Torres de María, O., Abril, R.J. & Casp, V.A. 2002. Determinación de las propiedades de un hielo líquido formado a partir de agua y NaCl. Estudio teórico - experimental. *Actas del 2° Congreso Español de Ingeniería de Alimentos [CD-Rom]. Lleida: Universitat de Lleida.* ISBN 84-8409-162-7.

Smith, M.W. & Tice, A.R. 1988. Measurement of the unfrozen water content of soils: a comparison of NMR and TDR methods. *In Proceedings of the 5th International Conference on Permafrost:* 473-477.

van Genuchten, M.T. 1980. A closed-form equation for predicting the hydraulic conductivity of unsaturated soils. *Soil Science Society of America Journal* 44(5): 892-898.

Watanabe, K. & Mizoguchi, M. 2002. Amount of unfrozen water in frozen porous media saturated with solution. *Cold Regions Science and Technology* 34: 103-110.

Watanabe, K. & Wake, T. 2009. Measurement of unfrozen water content and relative permittivity of frozen unsaturated soil using NMR and TDR. *Cold Regions Science and Technology* 59(1): 34-41.

Williams, P.J. 1964. Unfrozen water content of frozen soils and soil moisture suction. *Géotechnique* 14(3): 231-246.

Xiao, Z., Lai, Y. & Zhang, M. (2018). Study on the freezing temperature of saline soil. *Acta Geotechnica* 13(1): 195-205.

Zhou, X., Zhou, J., Kinzelbach, W. & Stauffer, F. 2014. Simultaneous measurement of unfrozen water content and ice content in frozen soil using gamma ray attenuation and TDR. *Water Resources Research* 50(12): 9630-9655.